The characteristics of sonoluminescence*

An Yu(安 宇)† and Zhang Wen-Juan(张文娟)

Department of Physics, Tsinghua University, Beijing 100084, *China*

(Received 17 May 2011; revised manuscript received 25 June 2011)

Cavitation luminescence is light emission from gases that are compressed to high temperature and high pressure inside a bubble or group of bubbles. The numerical simulation in this study indicates that if the temperature and pressure inside a bubble are not high enough, then dim and spectral line emission dominates. However, if the temperature and pressure inside the bubble are very high, then the light is bright and a continuum spectrum will be generated. Calculations of the spectrum using modified equations of bubble motion can simulate the spectral profile well. However, pulse width calculations using these equations only partly agree with the experimental results.

Keywords: sonoluminescence, spectrum, pulse width

PACS: 78.60.Mq, 32.30.–r, 33.20.–t **DOI:** 10.1088/1674-1056/21/1/017806

1. Introduction

Studies of single-bubble sonoluminescence (SBSL)[1,2] have achieved significant progress during the past 20 years. A gas bubble in a liquid is compressed by an acoustic wave with a frequency in the range 20–40 kHz. The gas is rapidly (in a few nanoseconds) heated to a high temperature (a few tens of thousands of degrees), and the bubble then flashes with each cycle of the driving acoustic wave. This is merely compressed hot gas light emission.[3−7] During the processes, noble gas rectification[8] occurs in the bubble. The gas is therefore primarily a noble gas in a mixture with the surrounding liquid vapor. Recent calculations[9,10] have revealed that as the maximum temperature inside the bubble approaches 10,000 degrees, molecular or atomic-line spectral emission dominates. Then, as the temperature increases further, emissions from bubbles of similar sizes become brighter, and the contribution from the continuum overwhelms the line spectra and dominates the light emission. Processes such as bremsstrahlung (electron–neutral atom, electron–ion) and recombination radiation, and the radiative attachment of electrons to atoms or molecules, contribute to continuum generation. Finally, as the temperature increases over a few tens of thousands of degrees, the electron–ion bremsstrahlung and recombination radiation overwhelm the other contributions, which agrees with the experimental observations of SBSL spectra.[11,12] In addition to the temperature, the pressure also affects whether the line spectrum is prominent. In this paper, we will present the simulation data to provide more concrete evidence for the above arguments.

Another goal of this study of SBSL spectra is to identify the correct form of the bubble motion equation from several candidates.[13−19] There are many slightly different forms of bubble motion equations, which are called Rayleigh–Plesset (RP) equations. These equations were derived using the low-speed assumption that the speed of the bubble wall is much smaller than that of the sound in the surrounding liquid. If we look at the motion of a sonoluminescing bubble during one period of the sound wave, this assumption is valid except during the short period (a few nanoseconds) when the bubble is compressed to its minimum size. In this case, the speed of the bubble wall is close to the speed of sound. Therefore, the equation may be invalid. To approximate the bubble motion, we need to extrapolate the RP equation to this moment, in which the low-speed assumption does not hold. Although it is very short, this is a critical period. It is the moment when the bubble flashes, and some most important hydrodynamic, thermodynamic or chemical processes occur during this period. The RP equations with slightly different forms give similar results for the bubble motion. However, for this short period, these variant forms yield very different hydrodynamic results.[20] This may result in the changes in the SBSL spectrum. By comparing the numerical calculations with the experimental data,

*Project supported by the National Natural Science Foundation of China (Grant No. 10974116).

†Corresponding author. E-mail: anyuw@tsinghua.edu.cn

© 2012 Chinese Physical Society and IOP Publishing Ltd

we can identify which equation is the best candidate for accurate reproduction of the experimental observations. Currently, the calculated spectrum does not rigorously reproduce the experimental data. However, the observed SBSL spectral profile can be estimated using this method.[9,10,21] In fact, to achieve a match between the calculation and experimental results, we need not only an accurate equation of bubble motion but also other parameters, such as the bubble size and the intensity of the driving acoustic wave. However, we were unable to find this data accompanied by observations of the SBSL spectrum in any previous reports. Fortunately, there is other information available. For example, in the case of SBSL bubbles in water, some spectra are almost featureless.[22] This type of emission spectra tends to come from bubbles with the brightest output. For stable SBSL bubbles, there is an upper threshold for their ambient radii R_0, and for the amplitude of the driving acoustic pressure $p_{\rm a}$.[23,24] The upper threshold of R_0 has been attributed to shape instability.[25] However, the upper threshold of $p_{\rm a}$ is caused by spherical asymmetrical perturbation of the acoustic pressure (about a few Pa).[26] Generally, when the upper threshold of $p_{\rm a}$ is approached, the bubble light emission reaches its brightest point and the continuum dominates its spectrum.

In addition to spectral effects, the calculated full width at half maximum (FWHM) of the SBSL pulse may also be affected by the bubble motion equation. The differences between the slightly different RP equations are accented as the bubble approaches its minimum size. Thus, when the bubble flashes, the calculated SBSL pulse width may differ according to the chosen RP equation. When compared with experimental results, this calculation may provide valuable information on the RP equation.

2. Theory and formulas

We developed a model to simulate the flash in a spherical bubble. We assumed that a mixture of inert gas and water vapor fills the bubble. In addition, the evaporation and condensation of water vapor occurs at the bubble wall, but the inert gas is confined to the bubble. Many properties were considered in the calculation, such as the viscosity, diffusion and thermal conduction of the gas. The heat exchange between the gas in the bubble and the surrounding water, chemical dissociation of hot gases and the ionization of atoms or molecules were also considered. Most of the important light emission processes in the hot gas (at temperatures of a few tens of thousands of degrees) are included in the model. These processes include the emission of atomic and ionic spectral lines of the inert gas,[27] molecular spectral emission of OH radicals near 310 nm, the radiative attachment of electrons to atoms or molecules, and bremsstrahlung (electron–neutral atom and electron–ion) and recombination radiation. These processes depend on the local pressure, density and temperature, which can be calculated by solving the partial differential equations for the fluid mechanics inside the bubble. The boundary is the moving bubble wall, and its motion can be described by the RP equation.[13−19] For details on this model, please refer to Refs. [6], [9], and [10].

The simple form of the RP equation[13−16] is as follows:

$$R\ddot{R}+\frac{3}{2}\dot{R}^2=\frac{1}{\rho_{\rm l\infty}}[p_{\rm l}-p_\infty-p_{\rm s}(t+t_R)]+\frac{t_R}{\rho_{\rm l\infty}}\dot{p}_{\rm l}, \quad (1)$$

where $R(t)$ is the radius of the bubble, $\rho_{\rm l\infty}$ is the ambient liquid density, p_∞ is the ambient pressure, $p_{\rm s}(t)=-p_{\rm a}\sin(\omega t)$ is the driving acoustic pressure, $t_R\equiv R/c_{\rm l\infty}$, with $c_{\rm l\infty}$ being the sound speed in the liquid at ambient temperature and pressure (1 atm, 1 atm $=1.01\times10^5$ Pa). $p_{\rm l}=p_{\rm g}(R,t)-4\eta\dot{R}/R-2\sigma/R$ is the pressure on the liquid side of the bubble wall, where $p_{\rm g}(R,t)$ is the pressure on the gas side of the bubble wall, η is the dynamic viscosity and σ is the surface tension coefficient of the liquid. Equation (1) may be modified in the low speed limit.[17−19] This is the case in which the speed of the bubble wall is much smaller than the speed of sound in the liquid. One modification is the Keller–Miksis form as[18]

$$\begin{aligned}&(1-M)R\ddot{R}+\frac{3}{2}\left(1-\frac{M}{3}\right)\dot{R}^2\\&=(1+M)\frac{1}{\rho_{\rm l\infty}}[p_{\rm l}-p_\infty-p_{\rm s}(t+t_R)]+\frac{t_R}{\rho_{\rm l\infty}}\dot{p}_{\rm l}, \quad (2)\end{aligned}$$

where $M\equiv\dot{R}/c_{\rm l\infty}$ is the bubble-wall Mach number, which includes the effects of liquid compressibility. Another modification employed in this work is the simple math approximation.[28] Because Eq. (2) is valid for the case $|M|<<1$, it is nearly equivalent to replacing $1\pm M$ with $\mathrm{e}^{\pm M}$ and $1-M/3$ with $\mathrm{e}^{-M/3}$.[29] This modified equation is

$$\begin{aligned}&\mathrm{e}^{-M}R\ddot{R}+\frac{3}{2}\mathrm{e}^{-M/3}\dot{R}^2\\&=\mathrm{e}^{M}\frac{1}{\rho_{\rm l\infty}}[p_{\rm l}-p_\infty-p_{\rm s}(t+t_R)]+\frac{t_R}{\rho_{\rm l\infty}}\dot{p}_{\rm l}. \quad (3)\end{aligned}$$

The advantage of this form is that the sign of any term in Eq. (3) does not change with the changes in M.

Equations (1)–(3) are valid for $|M| \ll 1$. However, it is unclear whether the equations are valid or not for $|M| \sim 1$. Unfortunately, in the case of SBSL, at the moment of the bubble flash $|M| \sim 1$, because the duration of $|M| \sim 1$ is short, we may extrapolate the RP equation or its modified form to this period. Furthermore, in Eqs. (1)–(3), we can simply replace $c_{\mathrm{l}\infty}$ and $\rho_{\mathrm{l}\infty}$ with c_{l} and ρ_{l}, respectively, where c_{l} and ρ_{l} are the sound speed and the liquid density on the liquid side of the bubble wall, respectively. These values can be determined using the Tait equation, and this modification makes the extrapolation of the equation to the $|M| \sim 1$ period more reasonable.[30] Though there are many other possible modifications,[17–19,28] we consider only these six cases, namely Eqs.(1)–(3), and the three corresponding modified equations, in which $c_{\mathrm{l}\infty}$ and $\rho_{\mathrm{l}\infty}$ are replaced with c_{l} and ρ_{l}, respectively. For simplicity, we call Eq. (1) RP, Eq. (2) KM, and Eq. (3) KM_EXP, and their modified versions are MRP, MKM and MKM_EXP, respectively.

3. Numerical results and discussion

3.1. The contribution percentage of the spectral lines and continuum

Experiments[11,12,31] and simulations[9,10,32] have shown that the spectral lines in the SBSL spectrum are prominent for dim bubbles, but broaden into the continuum background for bright bubbles. From this, it is apparent that there is a connection between the spectral profile and the conditions inside the bubble as it flashes. To verify this, we use the maximum temperature inside the bubble at its minimum size and the corresponding pressure to approximate the extreme conditions inside the bubble. Furthermore, two new quantities are introduced to describe the characteristics of SBSL. First, to represent the contrast of the spectral line and its continuum background, we define

$$\alpha = \frac{I_{\mathrm{line}} - I_{\mathrm{bg}}}{I_{\mathrm{bg}}}, \tag{4}$$

where I_{line} and I_{bg} are the intensities of the most prominent spectral line and its continuum background, respectively. Second, to calculate the contribution of the spectral lines, we define

$$\beta = \frac{N_{\mathrm{lines}}}{N_{\mathrm{tot}}}, \tag{5}$$

where N_{lines} and N_{tot} are the line emission and total photon numbers, respectively. For every sonoluminescing bubble, the maximum temperature of the bubble is reached at its minimum size and the corresponding pressure constructs a phase space where α or β is calculated. This phase diagram can be used to connect the SBSL spectral profile to the extreme conditions inside the bubble.

Figure 1 shows a phase diagram of an Ar bubble in water with a radius of 4.5 μm. Generally, if α is less than 20%, the spectral line on the continuum is significantly broadened. In Fig. 1, cases with significantly broadened spectral lines are concentrated in the high temperature and high pressure area. However, for cases with $\alpha > 100\%$, very clear spectral lines are concentrated at low temperatures (< 20000 K) and pressures ($< 10^5$ atm). For Xe bubbles, only the OH molecular lines near 310 nm are considered in the calculation of α. This result is similar to what is found for Ar bubbles (see Fig. 2). In fact, the result is independent of the type of inert gas filling the bubble. This calculation also reveals how α depends on the luminance of SBSL. The luminance of the bubble is proportional to its emitted photon number per flash. Figure 3 shows that α decreases as the bubble becomes bright, which agrees with the experimental observations. The calculation of β shows the same trend. Figure 4 shows that the emission of light contributed to the spectral line decrease with increasing bubble luminance. Therefore, for bright bubbles, the contribution coming from the continuum is dominant, and for dim bubbles, the line emission dominates. The phase diagrams of β and α show the same results (see Figs. 1 and 5). We can estimate the temperatures and pressures inside the bubbles through observation of their SBSL spectra. To explain the above arguments visually, we select three typical cases, which are shown in Fig. 5 (circled points), and their corresponding spectra are shown in Fig. 6. Note that the contribution from the radiative attachment of electrons to atoms or molecules is overestimated in Ref. [6]. In fact, it is similar to the contribution from the bremsstrahlung (electron–neutral atom, electron–ion) and recombination radiation for dim bubbles (see curve a in Fig. 6), but is negligible for bright bubbles (see curves b and c in Fig. 6). The atomic lines in the range 600–900 nm

for the dim Ar bubble should have been observed in the experiment. Unfortunately however, in that experiment the observation was restricted to the range 270–500 nm.[11] In addition, SBSL has been simulated in sulfuric acid. These cases showed similar trends to those in water.[10] In fact, cavitation luminescence is also the light emission of gases which are compressed to high temperature and pressure inside a bubble or group of bubbles. The calculated results revealed that the light emission characteristics of the bubble are independent of the ambient liquid, the type of driving force (acoustic wave or other mechanical fluid motion), or whether the bubble is isolated or in a group.

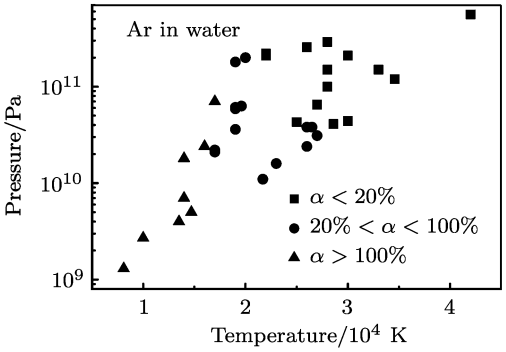


Fig. 1. Calculated phase diagram of α in the phase space formed by the maximum temperature of an Ar bubble at its minimum size, and the corresponding pressure.

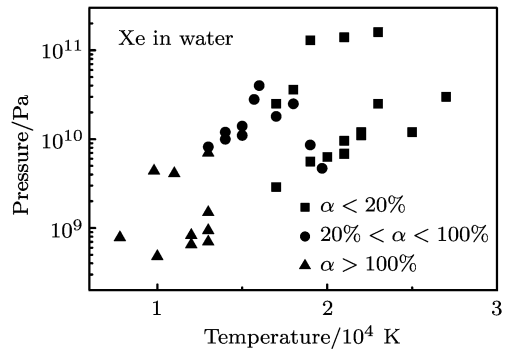


Fig. 2. Same as Fig. 1, but for Xe bubbles, and only OH molecular lines near 310 nm are considered in the calculation of α.

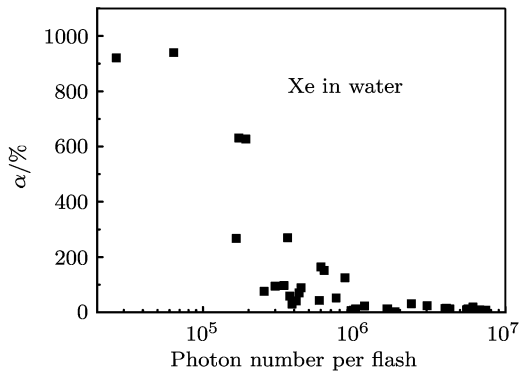


Fig. 3. Calculation of α versus the photon number per flash from an Xe bubble with a radius of 4.5 μm.

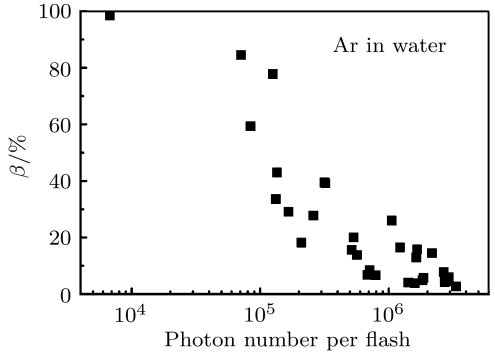


Fig. 4. Calculation of β versus the photon number per flash from an Ar bubble with a radius of 4.5 μm.

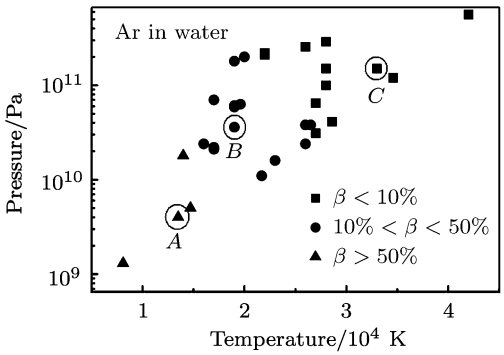


Fig. 5. Calculated phase diagram of β in the phase space formed by the maximum temperature of an Ar bubble at its minimum size, and the corresponding pressure.

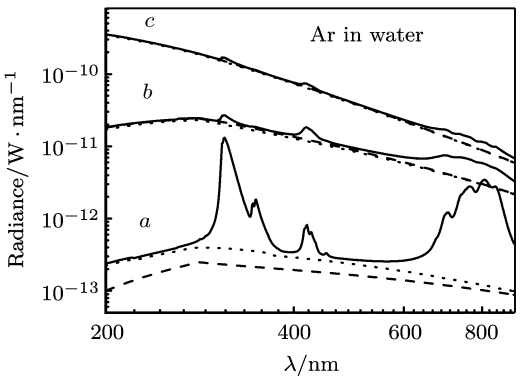


Fig. 6. Calculated spectra of an Ar bubble, where curves a, b and c correspond to the circled points A, B and C in Fig. 5, respectively. Each point corresponds to three curves in this figure. The dashed lines only considered contributions from the bremsstrahlung (electron–neutral atom, electron–ion) and recombination radiation. We then superadded the contribution from the radiative attachment of electrons to atoms or molecules to obtain the total continuum (dotted lines). Solid lines are the total of the continuum and the spectral lines.

3.2. RP equations

In the R_0–p_a parametric space, there is a stable SBSL region. We choose the case of bright SBSL bubbles because their spectra are usually featureless. In

0°C or room temperature water, if the expansion ratio of an Ar bubble is larger than eight, then the bubble is bright because the number of photons per flash reaches 5×10^5.[22] In this study, we consider bubbles with $R_0 = 4.5$ μm in 0°C and 20°C water, driven by an acoustic wave with a frequency of $f = 31.9$ kHz and $f = 33.8$ kHz, respectively. For these calculations $p_a = 1.4$ atm. All six equations yield almost the same bubble radius and expansion ratio $R_m/R_0 > 9$, where R_m is the maximum radius of the bubble. Therefore, experimentally, it should be a bright bubble and its spectrum should be featureless. However, the numerical results using the six equations are very different. In fact, we found that the deviation primarily comes from their extrapolation for the $|M| \sim 1$ case. This is the moment when the bubble is violently collapsing. Therefore, the density and the speed of sound of the surrounding liquid increase rapidly. To identify the best equation for this extrapolation, we compared their results with the experimental data.

Figure 7 shows the calculated spectra of the Ar bubble in water for the six equations. We then qualitatively compared these spectra with the observed one (Figs. 54–56 in Ref. [22]). It can be seen that the

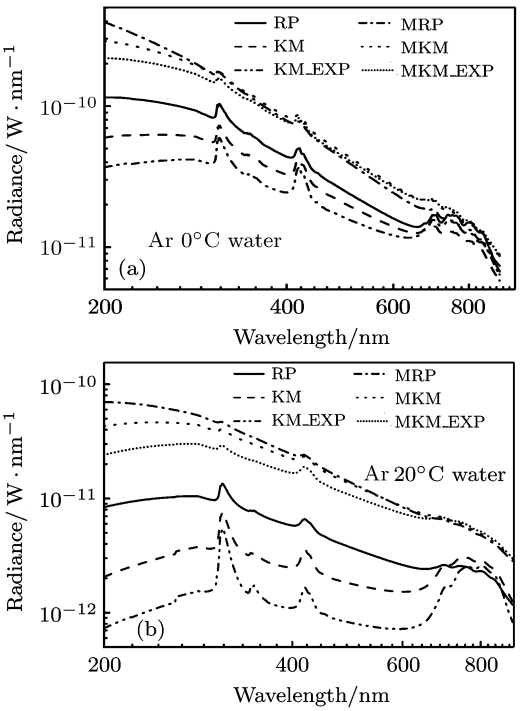


Fig. 7. Calculated Ar-bubble spectra using the six different RP equations: (a) in 0°C and (b) in 20°C water.

spectra produced using equations MRP, MKM and MKM_EXP are similar to the experimental observations. However, in the other equations, the spectral lines are unduly prominent. The equation should also be accurate for other gases. We therefore applied the modified equations to Xe bubbles. There is usually a maximum at the vicinity of 300 nm in the experimental spectrum of Xe bubbles.[22] In this sense, the spectrum obtained using MKM_EXP is more similar to the experimental curve (see Fig. 8). On the other hand, the spectral lines calculated using MKM_EXP and MRP are more prominent than those of the experimental data. Although we have combined this data with that of the He bubble calculation (see Fig. 9), it is still difficult to identify the best equation. Therefore, we need to investigate another characteristic of SBSL, namely the pulse shape.

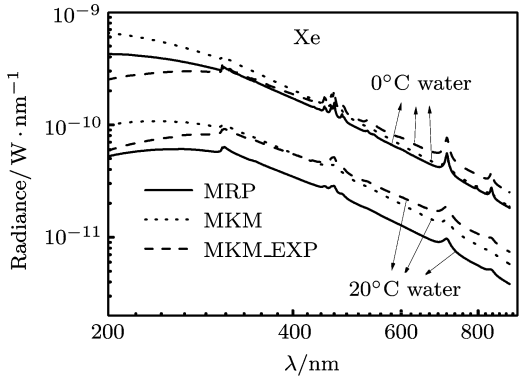


Fig. 8. Calculated Xe-bubble spectra using the three different RP equations.

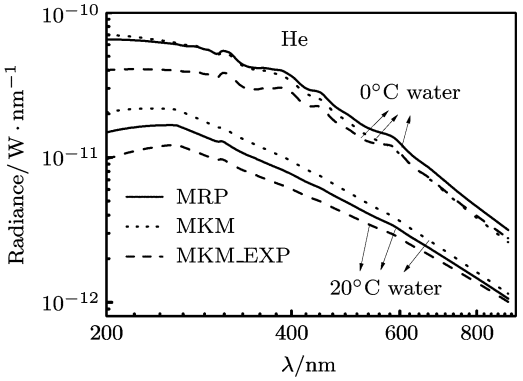


Fig. 9. Calculated He-bubble spectra using the three different RP equations.

The pulse shapes produced using the three equations are very different. For the Xe bubbles in 0°C water, the pulse widths produced by MKM and MRP are about 200 ps (FWHM). However, MKM_EXP produces a pulse that is too wide. The calculated data show that it is an interreflection of shock waves between the bubble center and the wall that result in the twin-peak shape (see Fig. 10(a)). In 20°C water, the pulse width generated using MKM_EXP is about 130 ps, which is reasonable. However, the pulse widths produced using the other two equations are too narrow

(see Fig. 10(b)). Furthermore, when the calculated FWHMs are compared (see Fig. 11) with the experimental results (Fig. 2 in Ref. [33]), we find that the calculated FWHMs for all the He and Ar bubbles are too small. Though the calculation of the SBSL spectra using MRP, MKM and MKM_EXP may approximate the experimental results, the calculated SBSL pulses do not always agree with the experimental observations. On the other hand, we find that the equation of state of gases has little effect on the optical pulse shape. In our model, we employed the van der Waals equation,[6] which is a good approximation except in the case where the gas volume is compressed to the van der Waals hard core volume. In this extreme case, the numerical calculation is invalid. Figure 12(a) represents the calculated temperature and the van der Waals hard core $\Sigma\nu_i b_i$ when the bubble turns to its minimum size, where ν_i is the ith gas mole number and b_i is its van der Waals hard core mole volume. We see that the extreme case of $\Sigma\nu_i b_i \sim 1$ only appears in the vicinity of the bubble wall, where to make the numerical calculation proceed, we set $\Sigma\nu_i b_i = 0.97$ if $\Sigma\nu_i b_i > 0.97$ (see curve b in Fig. 12(a)). Fortunately, at the bubble wall, the temperature is too low to affect the light emission processes (see curve a in Fig. 12(a)). Thus, this treatment does not affect the accuracy of the calculation and only lasts a very short time. In addition, we find that the pulse shape is stable to the van der Waals hard core volume parameter. In the calculation, we try the numerical trial to adjust the van der Waals hard core volume of Ar gas as 10% more or 10% less than that from the experimental data. The results are similar (see curves a, b and c in Fig. 12(b)). Therefore, we doubt whether the discrepancies between the calculation and the experimental result for the optical pulse width raise from the inaccuracy of the RP equation as it is extrapolated to the $|M| \sim 1$ case. On the other hand, the homogeneous model ignoring the vapor effects can produce pulse width agreement with the experimental data,[5] where the RP equation had no problem, as it is extrapolated to the $|M| \sim 1$ case. Though it is apparent that the present model is more realistic than the homogeneous one, by comparing our results with the results in Ref. [5], we are now confused by the present simulation results.

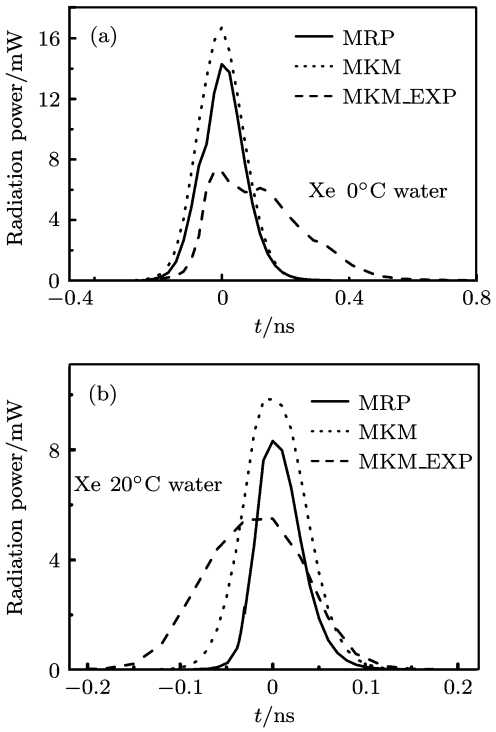


Fig. 10. Calculated Xe-bubble SBSL pulses using the three different RP equations corresponding to the cases in Fig. 8: in (a) 0°C and (b) 20°C water.

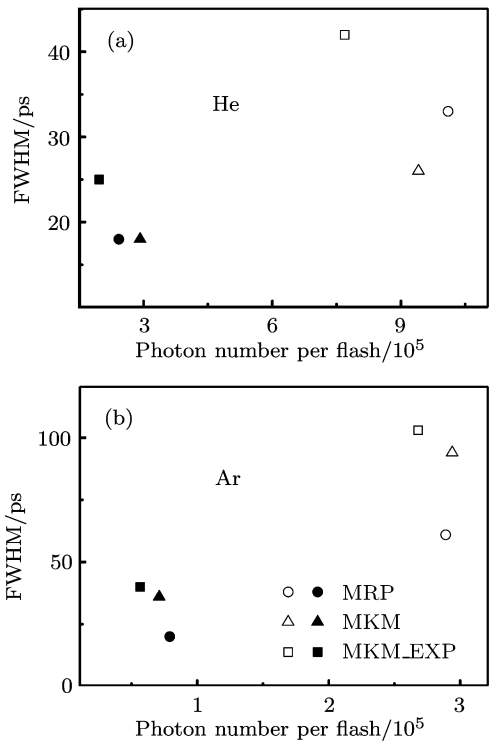


Fig. 11. Calculated FWHM versus photon number per flash using the three different RP equations. (a) Corresponding to the cases in Fig. 9 for the He bubble and (b) to three of the six cases in Fig. 7 for the Ar bubble. For 0°C water, hollowed points are used, and for 20°C water, filled points are used.

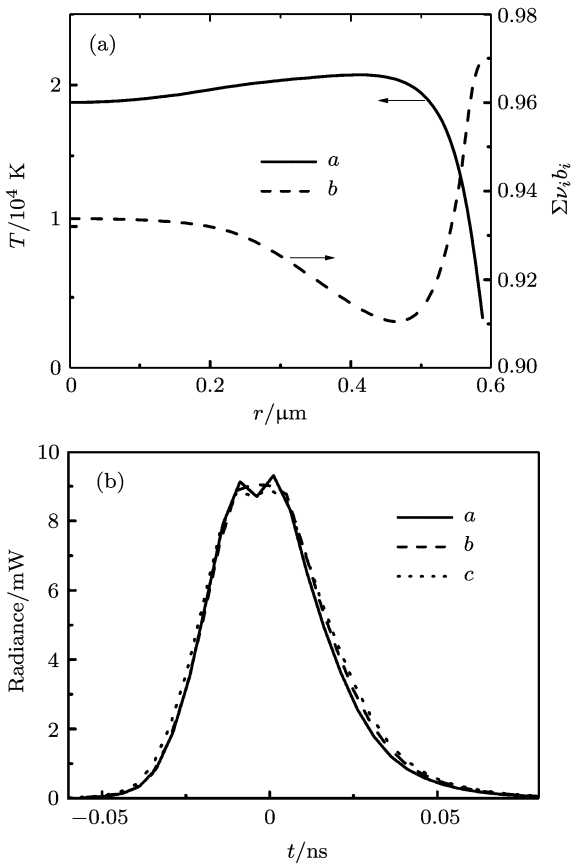


Fig. 12. For the Ar bubble in 20°C water: (a) the calculated temperature (curve a) and the van der Waals hard core $\Sigma\nu_i b_i$ (curve b) when the bubble is at its minimum size; (b) the optical pulses where the van der Waals hard core volume for Ar gas takes experimental data for curve b, while for curve a it is 10% more and for curve c 10% less than the experimental value.

4. Conclusion

We solved the partial differential equations for the fluid mechanics of two species, namely inert gas and vapor, in conjunction with the RP equation. We considered the processes of viscosity, thermal conduction, diffusion and gas–liquid phase transitions. Using the calculated pressure, density and temperature, we can evaluate the ionized electron density and the products of chemical dissociation. Simultaneously, ionization and chemical dissociation consume heat and change the molecular and atomic species of the gas, which leads to further correction of the temperature, pressure and density distributions. Then, we can evaluate the emission of light in high temperature and high pressure conditions. This gas radiation process includes the emission of atomic and ionic spectral lines of inert gas, the molecular spectral emission of OH radicals near 310 nm, the radiative attachment of electrons to atoms or molecules, and the bremsstrahlung (electron–neutral atom and electron–ion) and recombination radiation. Through analysis of the calculated data of the SBSL spectrum, we find that for dim bubbles, only low temperatures and pressures are reached; typically, below 20000 K and 10^5 atm for Ar. In these bubbles, molecular, atomic or ionic lines are the dominant contribution to their spectra. However, for the bright bubbles, very high temperature and pressure are approached, and thus the continuum radiation overwhelms the spectral line emission processes. Because this is a characteristic of high temperature and high pressure gas radiation, we conclude that this process is independent of ambient liquid type, cavitation cause and the number of bubbles that are sonoluminescing. The spectrum is only dependent on the gas species and the extreme conditions inside the bubble. However, the pulse shape depends on the duration of the extreme conditions inside the bubble. This is sensitive to the bubble motion equation.

Through calculation of the SBSL spectrum, we evaluated six different RP equations to identify the ideal equation for extrapolation to the $|M| \sim 1$ phase case. We found that the MRP, MKM and MKM_EXP equations seemed to be good candidates. However, further comparison of the calculated pulse duration indicates that they do not fully agree with the experimental results.

References

[1] Gaitan D F, Crum L A, Church C C and Roy R 1992 *J. Acoust. Soc. Am.* **91** 3166
[2] Barber B P and Putterman S J 1991 *Nature* **352** 318
[3] Frommhold L 1998 *Phys. Rev.* E **58** 1899
[4] Yasui K 1999 *Phys. Rev.* E **60** 1754
[5] Hilgenfeldt S, Grossmann S and Lohse D 1999 *Nature* **398** 402
[6] An Y 2006 *Phys. Rev.* E **74** 026304
[7] An Y 2011 *Sci. Sin. Phys. Mech. Astron.* **41** 343 (in Chinese)
[8] Lohse D, Brenner M P, Dupont T F, Hilgenfeldt S and Johnston B 1997 *Phys. Rev. Lett.* **78** 1359
[9] An Y and Li C 2008 *Phys. Rev.* E **78** 046313
[10] An Y and Li C 2009 *Phys. Rev.* E **80** 046320
[11] Young J B, Nelson J A and Kang W 2001 *Phys. Rev. Lett.* **86** 2673
[12] Chen W Z, Huang W, Liang Y, Gao X X and Cui W C 2008 *Phys. Rev.* E **78** 035301(R)
[13] Rayleigh L 1917 *Philos. Mag.* **34** 94
[14] Plesset M 1949 *J. Appl. Mech.* **16** 277
[15] Noltingk B and Neppiras E 1950 *Proc. Phys. Soc. London Sect.* B **63** 674
[16] Keller J B and Kolodner I I 1956 *J. Appl. Phys.* **27** 1152

[17] Gilmore F R 1950 Caltech Hydrodynamics Laboratory Report No. 26-4

[18] Keller J B and Miksis M 1980 *J. Acoust. Soc. Am.* **68** 628

[19] Prosperetti A and Lezzi A 1986 *J. Fluid Mech.* **168** 457

[20] An Y and Ying C F 2005 *Phys. Rev.* E **71** 036308

[21] Hammer D and Frommhold L 2002 *Phys. Rev.* E **65** 046309

[22] Barber B P, Hiller R A, Lofstedt R, Putterman S J and Weninger K R 1997 *Phys. Rep.* **281** 65

[23] Holt R G and Gaitan D F 1996 *Phys. Rev. Lett.* **77** 3791

[24] Gaitan D F and Holt R G 1999 *Phys. Rev.* E **59** 5495

[25] Hilgenfeldt S, Lohse D and Brenner M 1996 *Phys. Fluids* **8** 2808

[26] An Y, Lu T and Yang B 2005 *Phys. Rev.* E **71** 026310

[27] Ralchenko Y, Kramida A E, Reader J and NIST ASD Team 2008 *NIST Atomic Spectra Database* (version 3.1.5) Online: http://physics.nist.gov/asd3

[28] Prosperetti A and Hao Y 1999 *Phil. Trans. R. Soc. Lond.* A **357** 203

[29] An Y 2008 *Chin. Phys.* B **17** 2984

[30] Yuan L, Cheng H Y, Chu M C and Leung P T 1998 *Phys. Rev.* E **57** 4265

[31] Flannigan D J and Suslick K S 2005 *Nature* **434** 52

[32] Li C H and An Y 2009 *Sci. China Ser.* G **52** 593

[33] Hiller R A, Putterman S J and Weninger K R 1998 *Phys. Rev. Lett.* **80** 1090